Discovery of extraordinarily high-J OH in the HH 211 outflow

A. Tappe[1], C. J. Lada[1], J. H. Black[2], A. A. Muench[1]

ABSTRACT

We present a 5–37 μm infrared spectrum toward the southeastern lobe of the young protostellar outflow HH 211 obtained with the *Spitzer Space Telescope*. The spectrum shows an exceptionally rich sequence of highly rotationally excited OH ($v = 0$) emission. The highest excited rotational level has an energy $E/\mathrm{k} \approx 28000$ K above the ground level, which is, to our knowledge, by far the highest observed electronic ground-state excitation of OH in any astrophysical environment to date. In addition, we observe several pure rotational H_2O ($v = 0$) transitions, H_2 ($v = 0$) S(0) to S(7), HD ($v = 0$) R(3) to R(6), and atomic fine-structure lines from Fe^+, Si^+, S, and Cl.

Subject headings: ISM: Herbig-Haro objects — ISM: individual (HH 211) — ISM: jets and outflows — ISM: molecules — shock waves

1. Introduction

OH and H_2O are molecules of central importance to the interstellar oxygen chemistry in many diverse environments ranging from interstellar clouds to protoplanetary disks and comets. The main formation and destruction pathways of these species are now believed to be well established. However, their relative importance in a given astrophysical environment is generally poorly constrained due to a lack of suitable observations and the complex interaction of formation, destruction, and excitation mechanisms for H_2O and OH. Both molecules are expected to be abundant in hot gas owing to a series of neutral-neutral reactions whose activation barriers are overcome at high temperatures, and they act as important shock coolants due to their rich infrared spectra (e.g. Hollenbach & McKee 1979; Draine et al. 1983; Neufeld & Dalgarno 1989; Hollenbach & McKee 1989; Wardle 1999). *ISO* (Infrared Space Observatory), *SWAS* (Submillimeter Wave Astronomy Satellite), and *Odin* observations show enhanced OH and H_2O abundances in stellar outflows (e.g. Giannini et al. 2001,

---

[1]Harvard-Smithonian Center for Astrophysics, 60 Garden Street, MS-72, Cambridge, MA 02138; *atappe@cfa.harvard.edu*

[2]Onsala Space Observatory, Chalmers University of Technology, SE-439 92 Onsala, Sweden

Benedettini et al. 2002, Lerate et al. 2006, Persson et al. 2007, and Franklin et al. 2008), but were hampered by the large beam sizes that did not allow a detailed spatial analysis. In addition, observations with the *ISO* LWS (Long Wavelength Spectrometer) show only the lowest OH rotational states ($E/\mathrm{k} < 1200\,\mathrm{K}$) due to the wavelength coverage.

In this paper, we present the first detection of rotationally excited OH at previously unobserved high excitation levels in HH 211 with the *Spitzer Space Telescope* (Werner et al. 2004). HH 211, one of the youngest known stellar outflows, is a highly collimated, extremely high velocity (EHV) bipolar molecular outflow associated with a Class 0 protostar in the young stellar cluster IC 348. It has been studied in detail via excited H_2, CO, and SiO (e.g. McCaughrean et al. 1994; Gueth & Guilloteau 1999; Eislöffel et al. 2003; O'Connell et al. 2005; Caratti o Garatti et al. 2006; Tafalla et al. 2006; Lee et al. 2007).

2. Observations and data reduction

HH 211 was observed with the *Spitzer* IRS (Infrared Spectrograph, Houck et al. 2004) on 2007 March 12. We mapped the outermost region of the southeastern outflow lobe using the IRS short-low (SL2/SL1, 5.2–8.7/7.4–14.5 μm), short-high (SH, 9.9–19.6 μm), and long-high (LH, 18.7–37.2 μm) modules (see Fig. 1). The nominal spectral resolution is $R = 64$–128 as a function of wavelength for the low resolution and $R = 600$ for the high resolution settings. The total exposure times are 588 s for each SL, 720 s for the SH, and 600 s for the LH module. We also obtained IRAC (Infrared Array Camera, Fazio et al. 2004) and MIPS (Multiband Imaging Photometer for Spitzer, Rieke et al. 2004) image mosaics of HH 211 from the *Spitzer* data archive.

We performed the IRS data reduction consisting of background subtraction, masking of bad pixels, extracting the spectra, and generating the spectral line maps with CUBISM[1] v1.50 (Smith et al. 2007). We applied CUBISM's slit-loss correction function, and expect the absolute flux calibration of our spectrum to be accurate within 20%. A calibration to the observed MIPS 24 μm photometry is unreliable due to the strong line emission and the more than 2 year time difference between our IRS and the archival MIPS observations. We merged the extracted spectra of the individual IRS modules in SMART[2] (Higdon et al. 2004).

[1]http://ssc.spitzer.caltech.edu/archanaly/contributed/cubism/

[2]SMART was developed by the IRS Team at Cornell University and is available through the Spitzer Science Center at Caltech

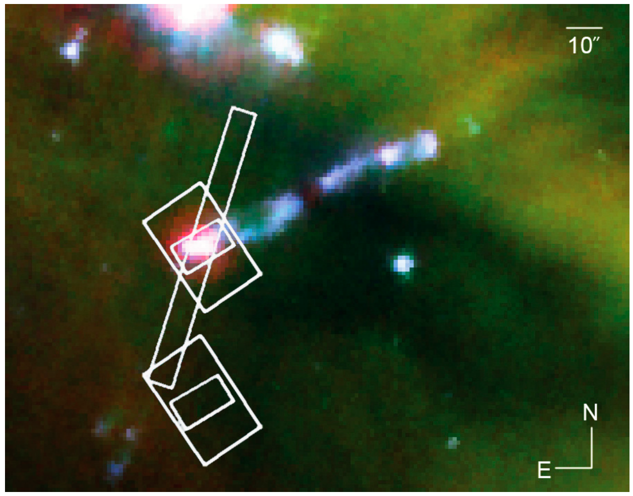

Fig. 1.— HH 211: *Spitzer* IRAC 3–9 μm+MIPS 24 μm color composite image (3.6+4.5 μm=blue, 8.0 μm=green, and 24 μm=red). White boxes outline the IRS SL, SH, and LH map coverage including the SH/LH background position (elongated, small rectangular, and large rectangular boxes, respectively). The image center coordinates are $3^{h}43^{m}56\overset{s}{.}8$, $32°00'34\overset{''}{.}4$ (J2000).

3. Results

The spectrum of HH 211 shows highly excited OH revealed by a sequence of pure rotational transitions spanning the complete $\Delta F = 0$, $\Delta J = -1$ $(v = 0)$ rotational ladders from $J' = 15/2$ to $69/2$ (Fig. 2 and 3). The highest excited OH transition has an upper state energy of $E/\,\mathrm{hc} = 19607\,\mathrm{cm}^{-1}$ $(E/\,\mathrm{k} \approx 28200\,\mathrm{K})$ above the ground level (see Fig. 4). Note that the population of the OH energy levels probably extends to even higher energies, but the corresponding rotational transitions fall in the wavelength range of the low resolution IRS modules below 10 μm. Due to the lower resolution, the SL modules are not sensitive enough to detect the faint, narrow emission lines. All OH $(\Delta F = 0)$ lines marked in Fig. 2 and 3 appear in pairs corresponding to the pure rotational $\Delta J = -1$ transitions in the two rotational ladders shown in Fig. 4. The additional energy level splitting due to Λ-doubling is only barely noticeable for the OH lines at the longest wavelengths in our spectra (see Herzberg 1971, for a detailed treatment of OH spectroscopy). Note that the $\Delta F = 1$, $\Delta J = 0, -1$ transitions connecting the two rotational ladders have orders of magnitude lower transition strengths. Nevertheless, we detect the two lowest excited OH $(\Delta F = 1$, $\Delta J = -1)$ lines with upper levels $J' = 7/2$ and $5/2$ $(E/\,\mathrm{k} \approx 620$ and $420\,\mathrm{K})$ at 28.9 and 34.6 μm, respectively, indicating a substantial population in the lower OH J-levels. We did not unambiguously detect any pure rotational OH transitions from excited vibrational levels.

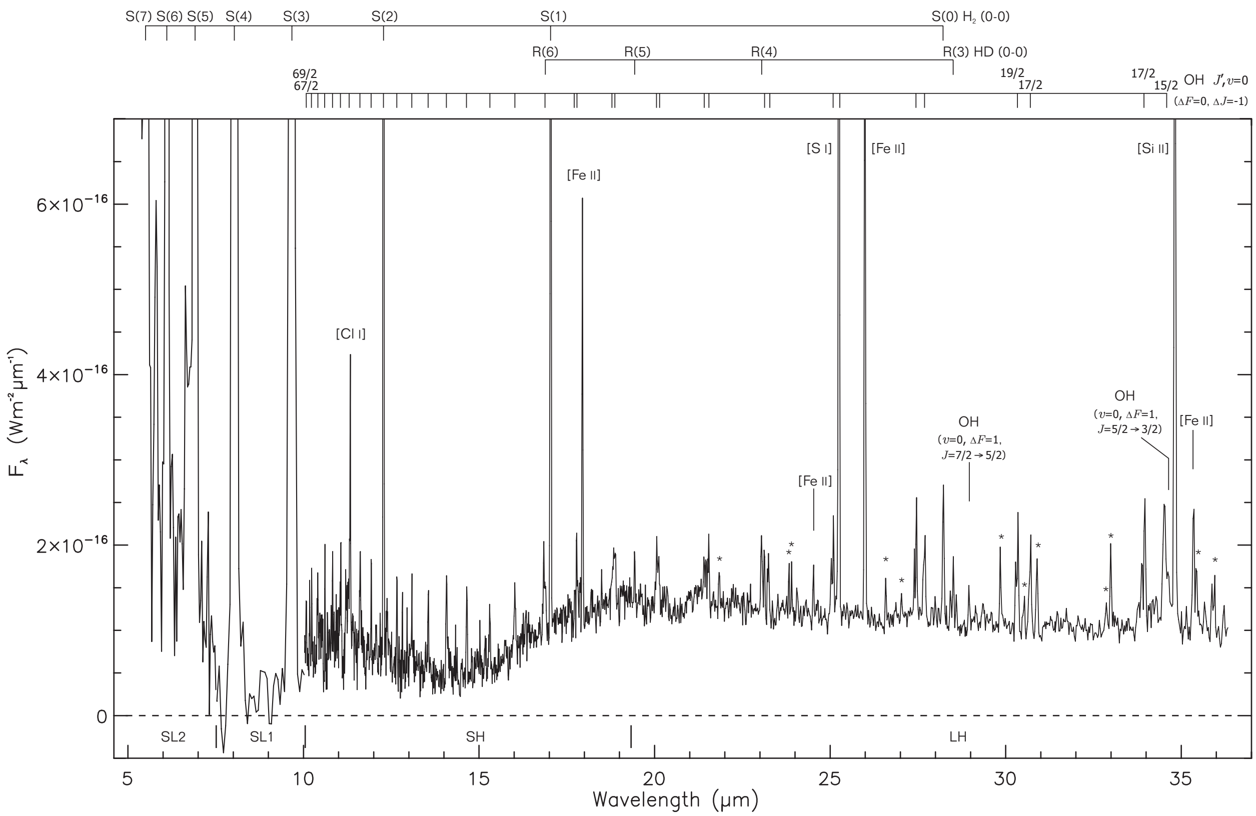

Fig. 2.— *Spitzer* IRS spectrum of the terminal shock in the southeastern HH 211 outflow lobe: All major detected lines are labelled, and the strongest water lines are marked with an asterisk. The strongest lines are clipped for illustration purposes. Note that the low resolution of the SL modules below 10 μm prevents the detection of narrow, faint lines (see Sect. 2). Fig. 3 shows a detailed view of the 10–20 μm region.

The low resolution portion of the spectrum is dominated by the strong, pure rotational H_2 (0–0) S(3)–S(7) transitions and the much weaker [FeII] 5.34 μm line. In addition to the previously mentioned OH lines, the high resolution portion longward of 10 μm shows H_2 (0–0) S(0)–S(2) including (1–1) S(3) at 10.18 μm, HD (0–0) R(3)–R(6), many H_2O ($v = 0$) pure rotational lines from energy levels between $E/\mathrm{k} \approx 935$ and 2350 K, and forbidden atomic fine-structure lines from Fe^+, Si^+, Ne^+, S and Cl. The spectrum also has noticeable continuum emission longward of 15 μm, which is fitted well by thermal dust emission at a temperature of about 85 K, represented by a modified blackbody with the Milky Way dust emissivities of Weingartner & Draine (2001). Two additional components at about 170 K and 30 K are needed to fit the complete continuum including the 8–15 μm region and the MIPS 70 μm flux of $F_\lambda = 1.1 \times 10^{-16}\,\mathrm{W\,m^{-2}\mu m^{-1}}$. There is also a strongly rising continuum shortward of 8 μm. The peculiar NIR continuum of HH 211 was previously noted by Eislöffel

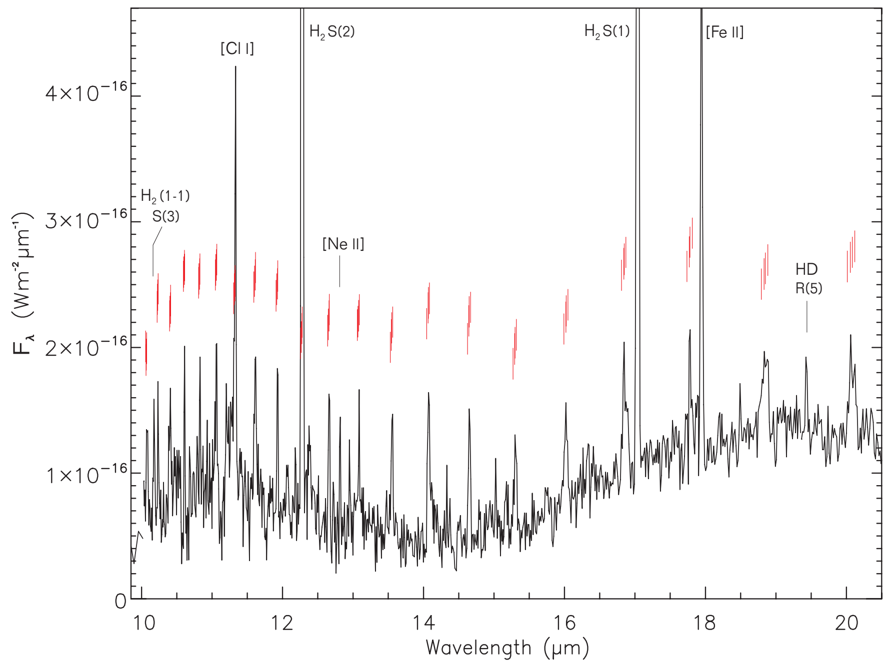

Fig. 3.— Detailed view of the OH ($v = 0$) $\Delta F = 0$, $J' = 29/2$ to $69/2$ lines between 10 and 20 μm from Fig. 2. Each unresolved OH line consists of 4 components (red ticks mark predicted line positions, see Sect. 3 for details). The broad, weak band near 11.3 μm is the PAH C–H bending mode, which is most likely a residue because of an incomplete background subtraction.

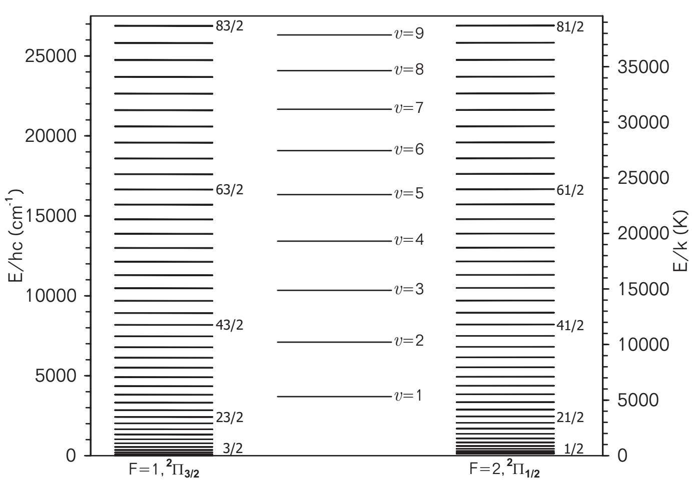

Fig. 4.— OH ($v = 0$) rotational energy levels in the $^2\Pi$ electronic ground state. The two rotational ladders result from the spin-orbit coupling of the unpaired $2p$ electron. All rotational levels are further split into Λ-type doublets with separations between 0.1 and 35.0 cm^{-1}, which are not visible on the scale of this plot (energy level data from Colin et al. 2002).

et al. (2003) and confirmed by O'Connell et al. (2005), who interpret it as scattered light from the protostar escaping along the low-density jet cavity.

A detailed discussion of the results with emphasis on the detected OH and H_2O emission and the origin of these molecules in shocks will appear in a forthcoming paper (Tappe et al. 2008).

This work is based on observations made with the Spitzer Space Telescope, which is operated by the Jet Propulsion Laboratory, California Institute of Technology under a contract with NASA. Support for this work was provided by NASA.

REFERENCES

Benedettini, M., Viti, S., Giannini, T., et al. 2002, A&A, 395, 657

Caratti o Garatti, A., Giannini, T., Nisini, B., & Lorenzetti, D. 2006, A&A, 449, 1077

Colin, R., Coheur, P.-F., Kiseleva, M., Vandaele, A. C., & Bernath, P. F. 2002, J. Mol. Spec., 214, 225

Draine, B. T., Roberge, W. G., & Dalgarno, A. 1983, ApJ, 264, 485

Eislöffel, J., Froebrich, D., Stanke, T., & McCaughrean, M. J. 2003, ApJ, 595, 259

Fazio, G. G., Hora, J. L., Allen, L. E., et al. 2004, ApJS, 154, 10

Franklin, J., Snell, R. L., Kaufman, M. J., et al. 2008, ApJ, 674, 1015

Giannini, T., Nisini, B., & Lorenzetti, D. 2001, ApJ, 555, 40

Gueth, F. & Guilloteau, S. 1999, A&A, 343, 571

Herzberg, G. 1971, The spectra and structures of simple free radicals. An introduction to molecular spectroscopy (Cornell University Press)

Higdon, S. J. U., Devost, D., Higdon, J. L., et al. 2004, PASP, 116, 975

Hollenbach, D. & McKee, C. F. 1979, ApJS, 41, 555

Hollenbach, D. & McKee, C. F. 1989, ApJ, 342, 306

Houck, J. R., Roellig, T. L., van Cleve, J., et al. 2004, ApJS, 154, 18

Lee, C.-F., Ho, P. T. P., Palau, A., et al. 2007, ApJ, 670, 1188

Lerate, M. R., Barlow, M. J., Swinyard, B. M., et al. 2006, MNRAS, 370, 597

McCaughrean, M. J., Rayner, J. T., & Zinnecker, H. 1994, ApJ, 436, L189

Neufeld, D. A. & Dalgarno, A. 1989, ApJ, 340, 869

O'Connell, B., Smith, M. D., Froebrich, D., Davis, C. J., & Eislöffel, J. 2005, A&A, 431, 223

Persson, C. M., Olofsson, A. O. H., Koning, N., et al. 2007, A&A, 476, 807

Rieke, G. H., Young, E. T., Engelbracht, C. W., et al. 2004, ApJS, 154, 25

Smith, J. D. T., Armus, L., Dale, D. A., et al. 2007, PASP, 119, 1133

Tafalla, M., Kumar, M. S. N., & Bachiller, R. 2006, A&A, 456, 179

Tappe, A., Lada, C. J., Black, J. H., & Muench, A. A. 2008, ApJ, submitted

Wardle, M. 1999, ApJ, 525, L101

Weingartner, J. C. & Draine, B. T. 2001, ApJ, 548, 296

Werner, M. W., Roellig, T. L., Low, F. J., et al. 2004, ApJS, 154, 1
